ELSEVIER

Catalysis Today 79–80 (2003) 97–103

CATALYSIS TODAY

www.elsevier.com/locate/cattod

A new reactor design for catalytic fluid–fluid multiphase reactions

Klaus-Diether Wiese*, Oliver Möller, Guido Protzmann, Martin Trocha

OXENO Olefinchemie GmbH, Paul-Baumann Strasse 1, D-45772 Marl, Germany

Abstract

The two-phase hydroformylation of lower olefins (Ruhrchemie–Rhône/Poulenc process) is a well known example of a multiphase fluid–fluid reaction (two liquid phases and a gas phase). Typically, reactions of this type are performed in stirred tank reactors. Investigation of the reaction in a packed tubular reactor revealed, that under very unconventional operation conditions space-time yields of 1-3 $\mathrm{t\,m^{-3}\,h^{-1}}$ are accessible. Compared to the conventional process, this is an increase by a factor of 10. This very surprising effect was clarified by simultaneous modelling of mass transfer and chemical reaction. Numerical simulations show that the effects are not due to a simple increase in mass transfer area. Alternative explanations are discussed. Further investigations in a mini pilot plant reveal a very simple yet highly efficient process design. Moreover, and in contrast to the conventional process higher olefins up to 1-octene can be converted to the respective aldehydes at reasonable space-time yields and with high selectivity. Successful application of the process principles to other fluid–fluid reactions suggests, that we have possibly found a more general concept for multiphase reactions.

Keywords: Catalytic fluid–fluid multiphase reaction; ahpha-Olefins; Two-phase hydroformylation; TPPTS; 1-Octene

1. Introduction

Homogeneous catalysis receives increasing attention since it offers some advantages over heterogeneous catalysis. The catalytic systems are clearly defined on the molecular scale and allow for a better theoretical understanding, the catalysts can be tailor-made by employing specific ligands, thus considerable higher activities and selectivities are accessible.

Conventionally, products and homogeneous catalysts are separated by distillation. Upon thermal stress, catalysts are very prone to decomposition. In application of expensive metals and ligands their loss has to be reduced to the lower ppb scale to keep the process economically efficient. Therefore, one of the key issues in homogeneous catalysis is minimisation of loss in catalyst recycle.

A promising approach is to fix the catalyst in a second fluid phase that is immiscible with the product, thus catalyst and product are easily separated by decantation. However, this requires a solvent system providing an appropriate phase behaviour. Recent developments are ionic fluids, mainly proposed by Wasserscheid and co-workers [1–4], besides fluorinated hydrocarbons are discussed [5–11]. These solvent systems are very interesting, still they are not applied in technology at the present time.

The concept of multiphase fluid–fluid reactions has been put into practice in Shell's SHOP process [12,13] for oligomerisation of ethene and in the Ruhrchemie–Rhône/Poulenc process [14,15] for hydroformylation of propene.

Hydroformylation is the most important homogeneous catalysed reaction conducted on commercial scale [16,17]. Olefins are reacted with synthesis gas to form aldehydes. In hydroformylation of short

---

* Corresponding author.

0920-5861/03/$ – see front matter © 2003 Elsevier Science B.V. All rights reserved.
doi:10.1016/S0920-5861(03)00015-4

chain olefins (propene, 1-butene) ligand modified rhodium is the most widely used catalyst. In the Ruhrchemie–Rhône/Poulenc process [14,15], a water soluble catalyst is used. Propylene, synthesis gas and aqueous catalyst solution are intensively contacted in a reactor by multiple stirrers. Internal heat exchangers are arranged to carry off the enormous heat of reaction. The reactor effluent flows into a separator. The light organic phase is further upgraded. The heavier catalyst phase is directly pumped back to the reactor. This smart process keeps thermal stress away from the catalyst. Additionally, phase separation takes place under synthesis pressure, thus rhodium remains protected by complex formation with carbon monoxide.

2. Theoretical considerations—the role of mass transfer in two-phase catalysis

2.1. Towards a new process

To improve the mass transfer in aqueous hydroformylation we went for a completely different technical approach. A tubular reactor equipped with internals (Sulzer SMV) was employed in place of a stirred vessel. The static mixers used provide a large surface, the hydrodynamic properties are very well investigated [18–21].

The catalyst phase is kept in large excess to the educts, high velocities are applied. Entering the reactor olefin and synthesis gas are finely divided by shear into droplets and small bubbles, respectively. By this means, a large surface for mass transfer is generated.

2.2. Mass transfer and chemical kinetics

For a description of the system, we used the stagnant film model. The specific diffusional mass transfer, J, of olefin molecules from the droplet via a laminar boundary layer to the catalyst phase is described by Eq. (1):

$$J = k_L a (c_O^0 - c_O) \tag{1}$$

The mass transfer is proportional to the specific surface area, a, of the droplets and the driving gradient of concentration. The proportionality constant, k_L, is the mass transfer coefficient of the catalyst phase. The product of both is referred to as $k_L a$ value.

The same considerations hold for mass transfer from the synthesis gas phase, either.

Application of the relevant dimensionless numbers (Sherwood, Reynolds, Schmidt, Weber) leads to the following expression:

$$Sh = f(Re, Sc) = k_1 Re^x Sc^y \tag{2}$$

$$k_L = \frac{Sh\, D}{d_H} = k_1 Re^x Sc^y \frac{D}{d_H} \quad \text{(for the mixer)} \tag{3}$$

The dimensionless diameter d_S/d_H is flow-dependent and thus a function of Re; d_S is the Sauter diameter of the droplets (or bubbles); d_H the hydraulic diameter of the mixer. The surface of each droplet is $6/d_S$ and the overall specific surface is obtained by multiplication by the hold-up of the dispersed phase φ:

$$\frac{d_S}{d_H} = f(Re, We) = k_2 Re^m We^n \tag{4}$$

$$a = \frac{6\varphi}{d_S} = \frac{6\varphi}{d_H k_2 Re^m We^n} \tag{5}$$

For Sulzer mixers, constants and exponents have been determined by evaluation of numerous liquid–liquid and gas–liquid systems [18–21].

Thus, mass transfer coefficient k_L and mass transfer surface a of gas and olefin phase, respectively, can be calculated. Multiplication and insertion of the dimensionless numbers yields the following expression for $k_L a$:

$$k_L a = \frac{0.177 \rho^{1.25} D^{2/3}}{\eta^{0.75} \sigma^{0.5}} \frac{1}{\varepsilon^{2.08} d_H^{0.42}} \frac{\varphi_O w_K^{2.08}}{\varphi_K^{0.85}} \tag{6}$$

Eq. (6) is arranged in three terms. The first term contains substance properties data, the second term characteristic data of reactor and its internals. The last term contains independent variables, i.e. hold-up of the dispersed phases φ and velocity of the continuous catalyst phase w_K. These variables can only be modified in the experiment directly. The substance property data can be obtained as a function of variables of state, pressure p and temperature T. The apparatus term contains known mixer properties. Combination with Eq. (1) leads to:

$$J = \frac{0.177 \rho^{1.25} D^{2/3}}{\eta^{0.75} \sigma^{0.5}} \frac{1}{\varepsilon^{2.08} d_H^{0.42}} \frac{\varphi_O w_K^{2.08}}{\varphi_K^{0.85}} (c_O^0 - c_O) \tag{7}$$

The reaction kinetics can be described by a conventional model [22] in Eq. (8).

$$r = k^0 e^{-E_a/RT} \frac{p}{1 + K_p p} c_K c_O \tag{8}$$

In the kinetic term the frequency factor k^0 and activation energy E_A are unknown. Commonly there is a linear relationship in catalyst concentration c_K. The Arrhenius equation should be valid for the temperature dependence of the rate constant k_R. For the sake of completeness the pressure dependence is expressed by an inhibition term, however, this is not relevant at the experimental conditions applied in the present work.

The actual olefin concentration c_O is at first unknown. By combining Eqs. (7) and (8) c_O can be eliminated, since mass transfer and chemical kinetics are connected.

3. Experimental

3.1. Experimental set-up

Fig. 1 outlines the experimental set-up. In place of a stirred vessel a tubular reactor filled with static mixers and a circulating pump are employed. The three phases are introduced to the reactor. After reaction the phases are separated and the catalyst is recycled to the reactor. Some typical data show the quite exceptional mode of operation:

- reactor length 3 m, diameter 17.8 mm, filled with Sulzer SMV mixers, internal volume about 0.56 l;
- catalyst mass flow up to 400 kg h^{-1};
- propene mass flow up to 3 kg h^{-1}, synthesis gas flow up to 1 kg h^{-1}.

By this means velocities up to 0.6 m s^{-1} and a residence time of about 5 s for chemical reaction, respectively, are accomplished.

4. Results

In the first experiments, the standard catalyst system (30 wt.% TPPTS, 800 wt. ppm Rh in pure water) was employed to determine the influence of mass transfer. The space-time yield was observed at different catalyst mass flows the feeding rate was kept constant (1.5 kg h^{-1} olefin, 1 N m^3 h^{-1} synthesis gas). As depicted in Fig. 2 a plot of the space-time yield as a function of $(w_K^{2.08}/\varphi_K^{0.85})$ exhibits a straight line in accordance with the model in Eq. (6).

At a low catalyst mass flow of 100 kg h^{-1}, the space-time yield is 0.17 t m^{-3} h^{-1}, a value that is usually observed in stirred vessels. With a rising catalyst mass flow the space-time yield increases to 0.92 t m^{-3} h^{-1} at 400 kg h^{-1}, which means an enhancement by a factor of 5.

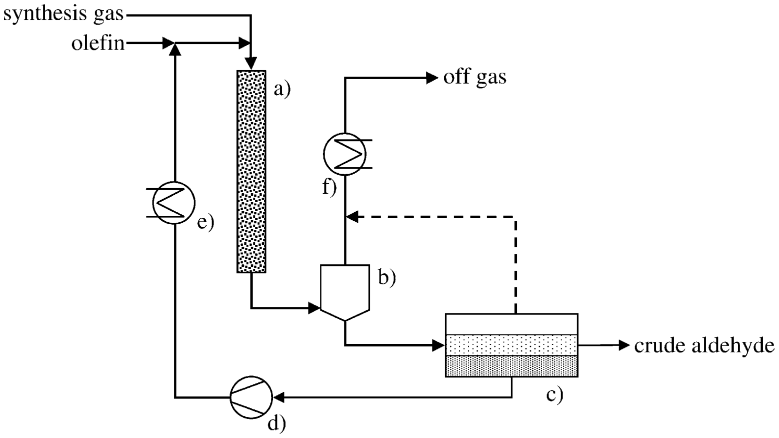

Fig. 1. Scheme of the aqueous hydroformylation mini plant: (a) tubular reactor, (b) gas flash, (c) settler, (d) circulating pump, (e and f) heat exchangers.

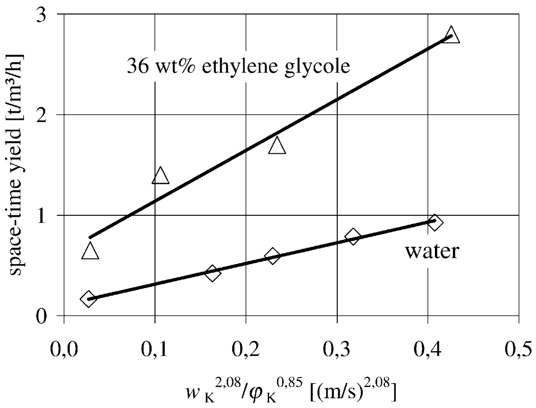

Fig. 2. Space-time yield at catalyst cycles w_K from 100–400 kg h^{-1} at 120 °C, 50 bar, 30 wt.% TPPTS, 800 ppm Rh, 1.5 kg h^{-1} propene, 1 N m^3 h^{-1} synthesis gas in water and 36 wt.% ethylene glycole.

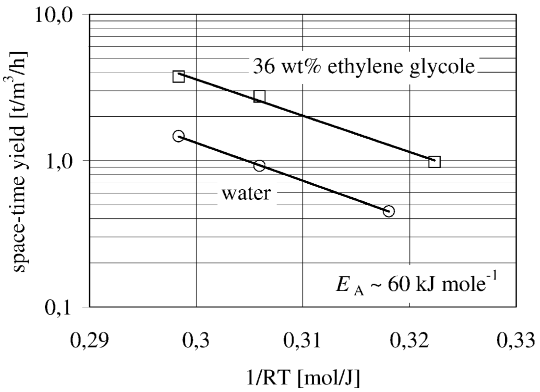

Fig. 4. Temperature dependence of space-time yield at 90–130 °C, 50 bar, 30 wt.% TPPTS, 800 ppm Rh, 2 kg h^{-1} propence, 0.8 N m^3 h^{-1} synthesis gas, 400 kg h^{-1} catalyst cycle, in water and 36 wt.% ethylene glycole.

The experiment in presence of ethylene glycole demonstrates a strong cosolvent effect. Again the space-time yield rises with the catalyst mass flow, the values are about four times those in the aqueous system.

Fig. 3 shows the dependence of space-time yield from propylene and synthesis gas hold-up, respectively, in the aqueous system. If, at a constant catalyst mass flow, the propylene hold-up is put up the space-time yield increases again. In contrast increasing the synthesis gas hold-up does not accelerate the reaction. There is even an adverse effect that can be explained by an increased drag-out of propene in the gas phase. We can conclude that only the mass transfer of propene determines the observable reaction rate.

Variation of the variables that have an effect on chemical kinetics reveals a completely different picture. The actual reaction rate is strongly temperature-dependent. From the Arrhenius plot in Fig. 4 an apparent activation energy of about 60 kJ mol^{-1} is derived, suggesting a kinetically controlled reaction. This is confirmed by the dependence of reaction rate from catalyst concentration depicted in Fig. 5. Over a large range a linear relationship is observed according to the kinetic model in Eq. (8).

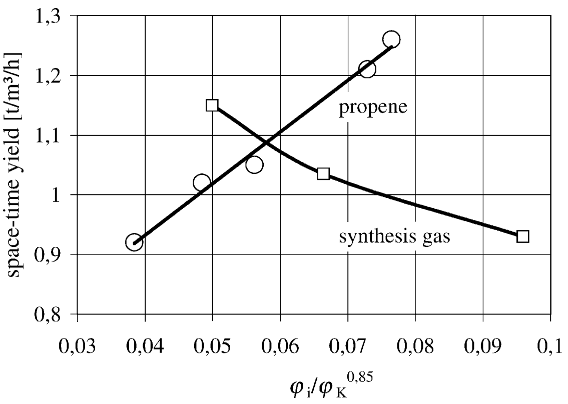

Fig. 3. Dependence of space-time yield on propene and synthesis gas hold-up at 120 °C, 50 bar, 30 wt.% TPPTS, 800 ppm Rh, 400 kg h^{-1} catalyst cycle in water.

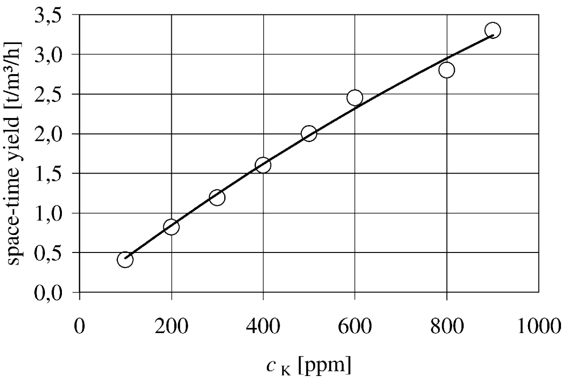

Fig. 5. Space-time yield at different Rh concentrations at 120 °C, 50 bar, 30 wt.% TPPTS, 1.5 kg h^{-1} propene, 1.0 N m^3 h^{-1} synthesis gas in 36 wt.% ethylene glycole.

5. Discussion—where does the reaction take place?

The experimental results presented in the previous section lead to an unequivocal conclusion. Mass transfer as well as chemical kinetics control the observed overall reaction rate.

The interaction of mass transfer and chemical reaction is intensively discussed in [23]. To compare mass transfer and chemical kinetics usually the Hatta number Ha is employed. Ha is the ratio of mass transfer induced by reaction and diffusion, respectively:

$$\mathrm{Ha} = \frac{\sqrt{k_\mathrm{R} D}}{k_\mathrm{L}} \qquad (9)$$

There are three distinct regimes. In case of $\mathrm{Ha} > 2$, (instantaneous reaction regime) the reaction proceeds completely inside the boundary layer. The mass transfer surface determines the actual reaction rate. On the other hand, at a very low Ha number $\ll 0.002$ mass transfer is negligible, the reaction rate is solely limited by chemical kinetics (kinetic regime). At a Ha number from 0.2 to 0.02 the reaction rate is almost completely determined by diffusion into the continuous phase via a boundary layer (diffusion regime). There are two transition regimes: The first between instantaneous and diffusion regime is characterised by the threshold values for Ha of 0.2 and 2, the second between diffusion and kinetic regime is characterised by Ha values from 0.002 to 0.02.

The experimental results suggest that mass transfer as well as kinetics play a decisive role. Therefore, the reaction must take place in one of the two possible transition regimes.

A differentiation between both cases is not possible, yet, since the actual rate constant inside the aqueous medium is not known. However the variables contained in the numerical model Eqs. (7) and (8) are all known except the rate constant, that is included in the Ha number. Therefore, introducing threshold values for Ha of the transition regimes allows for an estimation of the magnitude of the kinetic rate constant.

Increasing the cycle velocity and thus enhancing the mass transfer shifts the place of reaction from the interphase to the boundary layer. Introducing the threshold values of Ha (0.2 and 2) and the space-time yields determined experimentally lead to estimated rate constants that are about three orders of magnitude larger than that of the homogeneous reaction [24]. So the interphase and the boundary layer are very unlikely the place of reaction.

On enhancement of the mass transfer, the reaction changes from diffusion determined to kinetically determined. In other words, the place of reaction shifts from boundary layer towards bulk. An expression for the actual reaction rate is obtained by comparing diffusion and consumption by chemical reaction.

$$r_\mathrm{obs} = \left(\frac{1}{k_\mathrm{L} a} + \frac{1}{k_\mathrm{R}}\right)^{-1} c_\mathrm{O}^0 \qquad (10)$$

Eq. (10) again contains mass transfer coefficient as well as the kinetic coefficient. If the threshold Ha numbers (0.02 and 0.002) and the experimentally determined space-time yields are introduced, the rate constants obtained are in the same order of magnitude than in the homogeneous reaction [24]. From this considerations, it can be derived that in our experiments the reaction predominantly takes place in the bulk. We have observed a significant enhancement of the overall reaction rate compared to the stirred vessel. This suggests that in the vessel the reaction takes place between interphase and the boundary layer. This explanation agrees well with some results of Wachsen et al. [25]. From kinetic experiments at various hydrodynamic conditions in a stirred vessel the authors concluded that in their system the boundary layer is the place of reaction.

We have enhanced the overall reaction rate by shifting the place of reaction from the boundary layer towards the bulk and, thus increased the effectiveness factor of the catalyst phase. In the present reactor system the reduction of the thickness of the laminar boundary layer, i.e. the increase of mass transfer coefficients is crucial, in contrast to the stirred vessel, where the area of the boundary layer plays an important role.

We found an excellent agreement of experimental data and calculated values, giving evidence for the soundness of the applied model.

6. Towards application in technology

6.1. The technical solution

In order to design a plant another issue has to be considered. At high conversions the propylene hold-up becomes very small, thus the reaction rate decreases. However, there is a simple solution to this problem, since the high catalyst mass flow allows to employ a jet nozzle. By this means unconverted synthesis gas and propylene are recycled. The reactor can be operated at a partial conversion and a sufficient educt hold-up. Now, the accessible overall conversion is determined mainly by the quality of synthesis gas and propylene, only, as inert components have to be purged.

An important issue that has not been mentioned yet is the heat removal. Hydroformylation is a very exergonic process. In a stirred vessel high space-time yields would cause a run-away. Already the classical process employs internal heat exchangers. The large catalyst mass flow serves as a heat transfer fluid, the process is nearly isothermal. So heat exchangers can be arranged outside the reactor, simplifying the reactor design.

The high catalyst mass flow has even more advantages. The extremely short residence time of about $2\,\mathrm{s\,m}^{-1}$ diminishes the formation of secondary products like high boilers. By minimisation of the settler volume and the residence time of the organic phase selectivities of more than 99% are accessible.

6.2. Application of the technique to different reactions

A problem in hydroformylation in multiphase reaction systems is the strong decrease of solubility with growing chain length. Now, for the first time alpha-olefins up to 1-octene can be converted in a multiphase process [26] at reasonable space-time yields.

Additionally, we have studied the application to different reactions. The aldole cross-condensation served as an example for a two-phase liquid–liquid reaction [27]. Aldehydes can be reacted with acetone very selectively, illustrated by the production of 6-methyl-3-heptene-2-one as a precursor of isophytole. This is quite remarkable, since aldehydes usually are very prone to homocondensation.

The vinylation of longer chain carbon acids in the presence of their zinc salts by acetylene is an example of a gas–liquid reaction [28]. The temperature could be lowered by 40 °C, still the space-time yield was enhanced by a factor of three and the selectivity increased to 99%.

References

[1] P. Wasserscheid, W. Keim, Angew. Chem. Int. Ed. 39 (21)) (2000) 3772–3789.
[2] A. Jess, W. Leuchtenberger, W. Reschetilowski, P. Wasserscheid, Nachrichten aus der Chem. 48 (3) (2000) 359–363.
[3] W. Keim, D. Vogt, H. Waffenschmidt, P. Wasserscheid, J. Catal. 186 (2) (1999) 481–484.
[4] B. Driessen-Hölscher, P. Wasserscheid, W. Keim, CATTECH 2 (1) (1998) 47–52.
[5] A. Studer, S. Hadida, R. Ferritto, S.-Y. Kim, P. Jaeger, P. Wipf, D.P. Curran, Science 275 (5301) (1997) 823–826.
[6] I.T. Horvath, Acc. Chem. Res. 31 (10) (1998) 641–650.
[7] B. Cornils, Angew. Chem. Int. Ed. Engl. 36 (19) (1997) 2057–2059.
[8] W. Bannwarth, H.M. Glatz, M. Kohl, Manfred, D. Schwinn, C.C. Tzschucke, Bioforum 24 (11) (2001) 840–841.
[9] R.H. Fish, Chem. Eur. J. 5 (6) (1999) 1677–1680.
[10] I.T. Horvath, in: Book of Abstracts of the Proceedings of the 216th ACS National Meeting, Boston, 23–27 August 1998, FLUO-019, American Chemical Society, Washington, DC.
[11] I.T. Horvath, J. Rabai, Science 266 (5182) (1994) 72–75.
[12] D. Vogt, in: B. Cornils, W.A. Herrmann (Eds.), Applied Homogeneous Catalysis with Organometallic Compounds, vol. 1, Wiley–VCH, Weinheim, 1996, p. 251.
[13] D. Vogt, in: B. Cornils, W.A. Herrmann (Eds.), Aqueous Phase Organometallic Catalysis, Wiley–VCH, Weinheim, 1998, Chapter 7.1, pp. 541–547.
[14] C.D. Frohning, C.W. Kohlpaintner, in: B. Cornils, W.A. Herrmann (Eds.), Aqueous Phase Organometallic Catalysis, Wiley–VCH, Weinhein, 1998, Chapter 6.1.3.1, pp. 294–306.
[15] J. Herwig, R. Fischer, in: P.W.N.M. van Leeuwen, C. Claver (Eds.), Rhodium Catalyzed Hydroformylation, Kluwer Academic Publishers, Dordrecht, 2000, Chapter 7, pp. 189–202.
[16] G. Protzmann, K.-D. Wiese, Erdoel Erdgas Kohle 117 (59) (2001) 235–240.
[17] G. Protzmann, K.-D. Wiese, Petrole Tech 430 (2001) 49–55.
[18] F.A. Streiff, Mischen Kunstst. Kautschukprod (1993) 351–391.
[19] F. Grosz-Röll, J. Baettig, F. Moser, Verfahrenstechnik 17 (12) (1983) 698–707.
[20] G. Schneider, Inst. Chem. Eng. Symp. Ser. 121 (Fluid Mixing 4) (1990) 109–119.
[21] Sulzer, SMV Mischerpackungen für Extraktions und Reaktionskolonnen, Sulzer AG, 1986.
[22] C.D. Frohning, C.W. Kohlpaintner in: B. Cornils, W.A. Herrmann (Eds.), Applied Homogeneous Catalysis with Organometallic Compounds, vol. 1, Wiley–VCH, Weinheim, 1996, Chapter 2.1.1.3, pp. 44–60.
[23] J.-C. Carpentier, in: G. Agostino, P.L. Silveston (Eds.), Multiphase Chemical Reactors, Springer, Berlin, Chapter 2, pp. 32–80.
[24] P.C. d'Oro, L. Raimondi, G. Pagani, G. Montrasi, A. Andreette, Chim. Ind. 62 (7–8) (1980) 572–579.
[25] O. Wachsen, K. Himmler, B. Cornils, Catal. Today 42 (1998) 373–379.

[26] (a) K.-D. Wiese, G. Protzmann, J. Koch, D. Röttger, M. Trocha (Eds.), OXENO Olefinchemie GmbH, EP 1,057,524 (2000);
(b) G. Protzmann, K.-D. Wiese, W. Büschken, D. Röttger (Eds.), OXENO Olefinchemie GmbH, DE 199,57,528 (2001).

[27] (a) K.-D. Wiese, G. Protzmann, J. Koch, W. Büschken (Eds.), OXENO Olefinchemie GmbH, DE 199,57,522 (2001);
(b) G. Protzmann, K.-D. Wiese, W. Büschken (Eds.), OXENO Olefinchemie GmbH, EP 1,103,538 (2001).

[28] (a) K-D. Wiese, G. Protzmann, J. Koch, D. Röttger, M. Trocha (Eds.), OXENO Olefinchemie GmbH, EP 1,057,524 (2000);
(b) K.-D. Wiese, P. Olbrich, J. Gabriel (Eds.), OXENO Olefinchemie GmbH, DE 199,08,320 (2000).